*Work performed under the auspices of the U. S. AEC.
[1]W. Duane and R. A. Patterson, Proc. Natl. Acad. Sci. U. S. 6, 518 (1920); 8, 85 (1922).
[2]S. K. Allison and A. H. Armstrong, Phys. Rev. 26, 714 (1925).
[3]S. K. Allison, Phys. Rev. 30, 245 (1927); 32, 1 (1928).
[4]A. Jönsson, Z. Physik 36, 426 (1926).
[5]V. Hicks, Phys. Rev. 36, 1273 (1930).
[6]V. J. Andrew, Phys. Rev. 42, 591 (1932).
[7]M. Botzkes, Z. Physik 89, 667 (1934).
[8]S. I. Salem, R. T. Tsutsui, and B. A. Rabbani, Phys. Rev. A 4, 1728 (1971).
[9]L. Salgueiro, J. G. Ferreira, J. J. H. Park, and M. A. S. Ross, Proc. Phys. Soc. (London) 77, 657 (1960).
[10]J. H. McCrary, L. V. Singman, L. H. Ziegler, L. D. Looney, C. M. Edmonds, and C. E. Harris, Phys. Rev. A 4, 1745 (1971).
[11]R. W. James, *The Optical Principles of the Diffraction of X Rays* (Cornell U. P., Ithaca, N. Y., 1965).
[12]*International Tables for X-Ray Crystallography*, (Kynock, Birmingham, England, 1968), Vol. III.
[13]J. H. McCrary, L. D. Looney, C. P. Constanten, and H. F. Atwater, Phys. Rev. A 2, 2489 (1970).
[14]E. Storm and H. I. Israel, Nucl. Data Tables, A 7, 565 (1970).
[15]J. H. Scofield, Phys. Rev. 179, 9 (1969).

PHYSICAL REVIEW A VOLUME 5, NUMBER 4 APRIL 1972

Production (in Mg Vapor) and Loss (in H_2 Gas) of 1- to 42-keV/Nucleon $X\,^1\Sigma_g^+$ and $c\,^3\Pi_u$ Hydrogen Molecules*

Thomas J. Morgan,† Klaus H. Berkner, and Robert V. Pyle
Lawrence Berkeley Laboratory, University of California, Berkeley, California 94720
(Received 18 November 1971)

We have investigated collisions which result in the formation and destruction of the $(1s\sigma^2)X\,^1\Sigma_g^+$ ground state and the $(1s\sigma 2p\pi)c\,^3\Pi_u$ long-lived electronically excited state of molecular hydrogen. The molecules were formed by electron capture by 1- to 42-keV/nucleon H_2^+ or D_2^+ ions in Mg vapor. The resulting yields of $H_2(^1\Sigma_g^+)$, $H_2(^3\Pi_u)$, H, and H^+ are reported as a function of Mg-target thickness. Also reported are cross sections for total loss and ionization of the $^1\Sigma_g^+$ and $^3\Pi_u$ states of H_2 in collisions with H_2 gas.

I. INTRODUCTION

In recent years a large amount of experimental work has been devoted to measuring excited-state populations of energetic atomic-hydrogen and helium beams, and their destruction and formation cross sections. Much less is known about energetic excited-molecular hydrogen beams. The present work extends the field of measurement of keV-energy heavy-particle collisions involving excited states to the $n = 2$ united-atom equivalent state of molecular hydrogen. In this work we quantitatively analyze by beam-attenuation techniques the collisional formation and loss of the $(1s\sigma^2)X\,^1\Sigma_g^+$ ground state and the $(1s\sigma 2p\pi)c\,^3\Pi_u$ long-lived electronically excited state of energetic molecular hydrogen. The energy range of the present work is from 1- to 42-keV/nucleon. The H_2 molecules were produced from energetic H_2^+ ions by electron capture from H_2 or N_2 gas or from Mg vapor. According to the Massey hypothesis[1] the maximum cross section for charge exchange is large when the energy defect is small. (The energy defect is the difference between the internal energy of the initial and final states of the collision particles.) In the case of the charge-exchange process of interest in the present experiment, i.e., $H_2^+ + X \rightarrow H_2 + \cdots$, the energy defect for electron capture into $n = 2$ bound states of H_2 is about 4 eV for a Mg-vapor target and about 12 eV for a H_2 or N_2 gas target. Therefore, at low energies where the Massey criterion is valid, we expect Mg vapor to be a more effective charge-exchange medium for capture into excited states than H_2 or N_2 gas.

The desirability of metal vapors as charge-exchange media for the formation of excited hydrogen atoms has been experimentally verified by many groups (see, for example, Refs. 2–6). A theoretical survey of electron capture into excited states of atomic hydrogen by ground-state elements has been performed by Hiskes.[7] From these results Hiskes has estimated up to 50% electron capture into the $^3\Pi_u$ state of H_2 by passage of H_2^+ through Mg vapor.[8] Based on the above considerations, Mg vapor was used to attempt to enhance the $^3\Pi_u$ excited-state population of H_2 beams. In order to compare the metal-vapor results with common gases we also used H_2 and N_2 targets.

The experimental technique used for the analysis of the hydrogen molecules is the beam-attenuation technique introduced by Gilbody *et al.*[9] for metastable He atoms. Accurate absolute measurements can be obtained by this method only if a beam of fast projectiles contains sufficient excited particles, with long enough lifetimes and large enough cross sections to ensure observable changes in the colli-

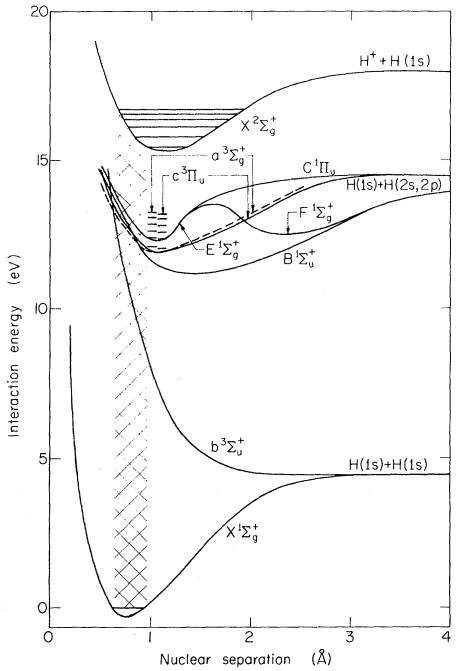

FIG. 1. Potential-energy diagram of H_2 and H_2^+ showing several excited states of H_2. The hatched area is the Franck-Condon classical region of transitions from the ground state ($v=0$) of H_2. Several vibrational levels are indicated by dashes. The potential-energy curves shown are based on calculations cited throughout this work.

sional attenuation of the beam when compared with a beam consisting almost exclusively of ground-state atoms or molecules. These conditions are satisfied in the present experiment for H_2 molecules.

We have measured the fraction of H_2 molecules that are produced in the $^3\Pi_u$ state by electron capture in Mg vapor at various target thicknesses.

We have also measured the total-loss cross sections ($H_2 \rightarrow H_2^+$, 2H, $H+H^+$, $2H^+$) and the ionization cross sections ($H_2 \rightarrow H_2^+$) for both the $^1\Sigma_g^+$ (ground) state and the $^3\Pi_u$ state in collisions with H_2 gas. Preliminary results were reported in Ref. 10.

II. HYDROGEN MOLECULE

The structure of the hydrogen molecule has been studied in detail both theoretically and experimentally (Herzberg[11] tabulated a large number of references on this topic up to 1950, and the present work contains a number of references since 1950). Figure 1 shows the potential energy curves for the electronic states of H_2 and H_2^+ that are of interest in this work.

The molecule contains two independent emission spectra: a triplet spectrum due to the two electron spins of the molecule being aligned, and a singlet spectrum due to electronic states with opposed electron spins. Spontaneous radiative transitions between these two term schemes is strictly forbidden by the selection rule on the total electron spin of the molecule, i.e., $\Delta S = 0$. An elaborate treatment of transitions in diatomic molecules is given by Herzberg.[11] Also, a concise and useful summary of selection rules is given by Garstang.[12]

In order to interpret the results of the present experiment, an understanding of the electronic states of the H_2 molecule is necessary. In Appendix A we present the results of a survey of the pertinent electronic excited states of H_2 and their lifetimes, and discuss which excited states have lifetimes greater than the time of flight of the H_2 molecule in the present experiment ($0.29 \leq t \leq 0.53$ μsec). Based on the discussion in Appendix A, we conclude that decay of all excited states, except the hydrogenlike (Rydberg) states with $n \gtrsim 8$, the $F\,^1\Sigma_g^+$ state, and the $c\,^3\Pi_u$ state, has taken place in this time interval.

First we consider the population of the hydrogenlike (Rydberg) states with $n \gtrsim 8$. From measurements by Kingdon *et al.*[13] and Solov'ev *et al.*[14] we conclude that less than 2% of the H_2 formed by electron capture by H_2^+ in Mg at 40 keV is in hydrogenlike states with $n \gtrsim 8$. This is negligible compared to the observed excited state fractions of 28% at this energy.

We do not know the relative populations of the $F\,^1\Sigma_g^+$ and $c\,^3\Pi_u$ states. However, when we consider the electron-capture process, we conclude from Fig. 1 that the $F\,^1\Sigma_g^+$ population should be negligible. The population distribution of the vibrational levels of H_2^+ ions from which the H_2 beam is prepared is determined by the vibrational distribution of the H_2 gas and by the energy of the electrons in the ion source. Since the energy separation between the first two vibrational levels of H_2 is ~ 0.4 eV, essentially all of the H_2 gas molecules were in the lowest vibrational level. Based on the Franck-Condon principle (i.e., the time required for an electronic transition is small compared to the nuclear motion of the molecule, so that the initial and final states have almost the same internuclear separation), the H_2^+ ions formed by electron ionization in the source will be almost exclusively in levels $v \leq 5$ (see Fig. 1).[15] When these H_2^+ ions capture an electron, we see from Fig. 1 that the range of nuclear separations (not indicated in the figure) defined by the Franck-Condon principle covers most of the $c\,^3\Pi_u$ state but only a small part of the $F\,^1\Sigma_g^+$ state. We therefore expect poor overlap with the F state in the capture process. Furthermore, from simple statistical arguments, we would expect a greater probability for capture into a triplet state relative to a singlet state. We therefore exclude the possibility of a significant population of the H_2 beam being in the $F\,^1\Sigma_g^+$ state, and we attribute the experimental observations of excited H_2 to the $c\,^3\Pi_u$ state.

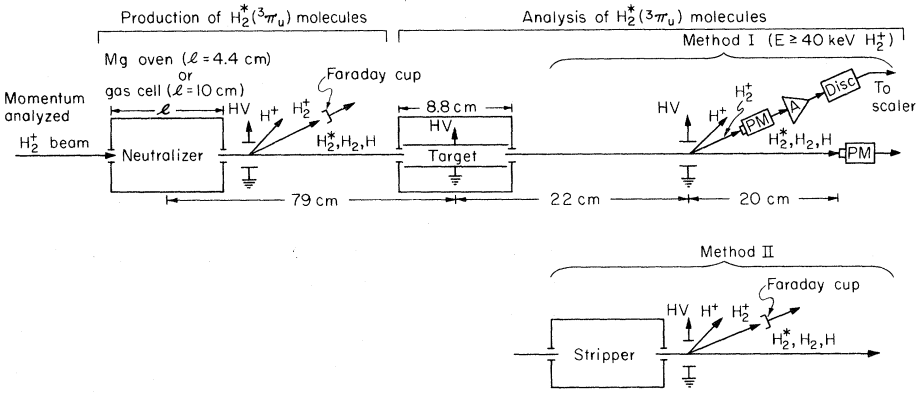

FIG. 2. Diagram of the experimental arrangement.

Unfortunately, there exists the nonradiative mechanism of predissociation in the case of the $^3\Pi_u$ state (see Appendix A). For the conditions of our experiment approximately one-half of the $^3\Pi_u$ rotational-state population will be subject to allowed predissociation during their time-of-flight through the apparatus.

III. EXPERIMENTAL APPARATUS AND PROCEDURE

A. Approach

Figure 2 shows the experimental arrangement.[16] The energetic H_2 molecules were produced by electron capture when a momentum-analyzed beam of H_2^+ ions traversed a neutralizing cell of Mg vapor, or H_2 or N_2 gas. (We have made measurements with incident H_2^+, D_2^+, and HD^+ ion beams. When the results are compared at the same velocity, they are the same within the experimental uncertainties.) Since we are investigating the H_2 molecule, the charged particles emergent from the neutralizer cell were swept out of the beam with an electric field, and the H_2^+ component, detected with a Faraday cup, was used to provide a monitor of the beam intensity.

The analysis of the H_2 beam was performed by beam attenuation. To this end the neutral beam, consisting of ground-state and excited H and H_2, traversed a target cell containing H_2 gas. We assume that the H_2 molecules are in either the $^1\Sigma_g^+$ ground state or in the $^3\Pi_u$ excited state (Sec. II). Since the collision cross sections of these two states are different, they attenuated differently upon traversing the target cell. By observing the emerging particles as a function of H_2 gas thickness in the target cell, we were able to deduce the total-loss and ionization cross sections for the $^3\Pi_u$ and $^1\Sigma_g^+$ states as well as the population of these states in the beam. By varying the neutralizer conditions, i.e., the type of neutralizer used (Mg, H_2, or N_2) and its thickness (atoms or molecules/cm^2), we were able to maximize the excited-state population or reduce it to an insignificant amount.

In order to increase the energy range of the measurements, two methods were used for particle detection. For method I (see Fig. 2) we employed particle-counting techniques: The particles were detected by CsI(Tl) crystals mounted on photomultipliers. Method I was limited to energies greater than about 10 keV/nucleon; below this energy it was difficult to resolve the pulse-height distribution of the atomic portion of the beam from the molecular portion. For method II a third gas cell (see Fig. 2), held at a constant pressure, was used to strip the fast molecules emerging from the target of an electron; the resulting H_2^+ current was measured with a Faraday cup. This method yields less information than method I but is applicable to total-loss cross-section measurements below 10 keV/nucleon. Using this method we have extended the total-loss cross-section measurements to 1 keV/nucleon.

B. Production of H_2 Molecules

The H_2^+ ions were produced in a PIG (Penning ionization gauge) ion source which could also be operated as an electron-gun source. The ions were accelerated electrostatically and momentum selected by a 90° analyzing magnet; they then passed through a 120-cm-long drift tube before entering the experimental region shown in Fig. 2. Measurements were made with accelerating voltages between 4 and 84 kV. The lower limit was determined by the performance of the detection system and the upper limit by our accelerator.

The accelerator voltage was measured by a high-impedance divider calibrated to ~1%. The uncertainty in the absolute value of the energy of the particles is estimated to be ~3%, except for energies less than 2 keV/nucleon, where it is estimated to be ~5%. This is based on the analysis of the deviation from linearity of a plot of the voltage necessary to deflect the particles versus the measured value of the accelerator voltage.

Just in front of the experimental region was an electromagnet that could be used to sweep the pri-

mary H_2^+ ions out of the beam path, so that the H_2 molecules produced by electron capture by H_2^+ from the background gas in the drift tube could be detected and subtracted as background. Under typical single-collision conditions in the neutralizer the background neutral production was $\lesssim 10\%$.

The Mg-vapor oven which served as the neutralizer cell has been described in Ref. 17. The entrance and exit collimator diameters were 0.508 and 1.27 mm, respectively. The effective length of the stainless-steel oven was 4.4 cm, measured from the entrance collimator to the exit collimator. An operating temperature of 665 K produced a Mg-vapor thickness of 1.75×10^{14} atoms/cm^2. A typical range of operation was from 616 to 783 K.

Before data were taken, the oven was outgassed at a temperature higher than that needed to produce the thickest Mg-vapor neutralizer of interest. This was done to ensure both the purity of the vapor and the proper interpretation of the vapor pressure. The temperature of the oven, which must be known in order to determine the Mg vapor pressure, was determined with two chromel-alumel thermocouples (with a zero-degree centigrade reference junction) connected to a potentiometer. To minimize radiative losses, the cell was surrounded by three layers of 0.25-mm-thick dimpled stainless steel. The calibration of the device was performed by Berkner *et al.*,[17] who originally used the oven as a collision cell for the measurement of electron-transfer cross sections of H and H^+ in Mg vapor. Data necessary for the calculations of the vapor pressure were obtained from Hultgren *et al.*[18] The assigned standard error in this Mg vapor pressure data is $\pm 10\%$.[17]

The H_2^+ component emergent from the neutralizer was deflected electrostatically 20° into a Faraday cup. The signal from the cup was sent to an electrometer whose output was fed to an integrator. This accumulated charge, which is proportional (for a given neutralizer thickness) to the number of neutrals incident on the target cell, was used to monitor the neutral beam.

Since the beam entering the target cell was 35 cm from the monitor Faraday cup, strict alignment was necessary to ensure correlation between the detected particles and the monitor, which were 82 cm apart. Alignment was performed visually with the aid of a telescope. Before taking data, the beam was tuned and maximized by observing the count rate due to the neutral particles. This count rate was then compared, as a function of the tuning parameters, with the electrometer output of the monitor Faraday cup. If the two signals were well correlated to within the uncertainty of visual meter observation, i.e., exhibited the same rise, plateau, and decrease in signal intensity as a function of the tuning parameters, data were acquired; if not, the beam was retuned. Occasionally realignment was necessary. The position of the beam was observed visually by replacing the Faraday cup with a phosphor-coated glass plate. The observed beam was much smaller than the Faraday cup diameter (2.54 cm). Permanent magnets were used to prevent electrons from entering or leaving the cup.

The neutral beam traveled 70 cm from the oven exit to the entrance of the differentially pumped target cell (see Fig. 2). The beam entrance and exit collimators were 3.30 and 4.31 mm in diameter, respectively, and 1.28 cm long. The effective length of the cell was 8.8 cm. This length was measured from the midpoint of the tubular entrance collimator to the midpoint of the tubular exit collimator (changes in the target thickness owing to gas in the surrounding tank of the target cell were inconsequential at all target pressures). The target cell was equipped with a pair of metal rods, ~0.5 cm apart, parallel to the beam line, which extended over the entire length of the cell. While measuring the H_2 attenuation, a voltage of 4 kV was applied to one of the rods in order to produce an electric field which ensured that the exiting H_2 beam was due only to attenuation, without the contribution of two-step processes, i.e., $H_2 \rightarrow H_2^+ \rightarrow H_2$. While measuring the ionization cross section, the voltage was turned off so that the H_2^+ component was allowed to leave the target cell and be detected. The pressure in the cell was measured by a Barocel capacitance manometer which had been calibrated numerous times over a period of several years by a McLeod gauge and an oil manometer.

C. Analysis of H_2 Molecules

1. *Method I: Single-Particle Counting*

After traveling 17 cm from the target-cell exit the H_2^+ component of the beam was bent 20° by the electric field between a set of deflection plates and traveled 24 cm further, where it was incident on a 2.54-cm-diam CsI(Tl) scintillation crystal which was mounted on an Amperex 10-stage XP-1010 photomultiplier tube (see Fig. 2). The neutral beam traveled 20 cm after leaving the deflector plates and was intercepted by a similar arrangement. The photomultiplier tubes were not cooled since upon cooling no significant increase in energy resolution was observed. The photomultiplier signal was amplified and shaped, discriminated, and finally scaled. A 400-channel pulse-height analyzer was used to set the upper and lower levels of the discriminators. A typical pulse-height spectrum, showing the resolution of the neutral components of the beam, is shown in Fig. 3.

Since the scintillator response (the number of photons produced per incident energetic particle) is proportional to the amount of energy transmitted

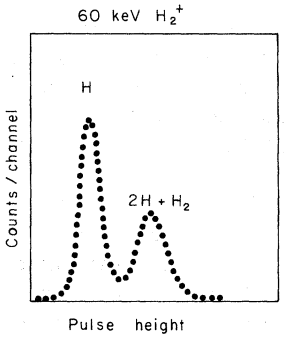

FIG. 3. Pulse-height spectrum obtained with a CsI(Tl) scintillation crystal for the neutral collision products of a 60-keV H_2^+ beam.

to the crystal during the impact of the energetic particle, two atoms, each of energy $\frac{1}{2}E$, whose difference in impact time is considerably shorter than the characteristic decay time of the crystal ($\sim 0.6\times10^{-6}$ sec), would be interpreted as a single particle of energy $\sim E$. Hence, in the present experiment, where the maximum possible difference in the impact time of the two H atoms produced by dissociation of H_2 in the target cell is $\sim 5\times10^{-9}$ sec, two H atoms could not be distinguished from an H_2 molecule.

The H atoms may, however, be spatially distinguishable by use of a low-transparency mesh. Assuming a random orientation of the H_2 internuclear axis with respect to the beam line and an isotropic angular distribution for the H atoms produced by dissociation, we have calculated for the case which produces the smallest scatter in the present experiment (42 keV/nucleon and ~2-eV dissociation energy) that, at the detector, the H atoms from dissociation in the target are uniformly distributed over a circular region with a 2.2-mm radius. The mesh, which had a transparency of ~1%, consisted of four layers of 22% transparent 2000-line/in. Cu Electromesh which had square apertures 6.35×10^{-3} mm on a side. Clearly, the grid size is significantly smaller than the majority of the H atom separations. The transmission was measured by using an H-atom beam. In order to identify the H_2 molecules from the (H+H) signal, the mesh was placed in front of the neutral detector. With the mesh in the beam line the probability of obtaining a full energy pulse from two simultaneous H atoms is $\sim 10^{-4}$, while the probability of obtaining a full energy pulse from a H_2 molecule is $\sim 10^{-2}$.

For each species of the beam detected (H_2^+, H^+, H_2, H), two sets of scalers were used to correct for random noise. By employing an incident H_2^+ beam, chopped at a frequency of 4.0 Hz by applying voltage to a set of steering deflector plates in the accelerator region, one set of scalers recorded the beam plus the noise and the other set recorded the beam-off signal (i.e., noise only), which was always much less than that of the beam-on signal. A set of timing scalers was used to determine the beam-on and -off counting times. Subtraction of the two time-normalized counts yielded the counts produced by the beam.

For this method, the ion source was operated in the electron-gun mode to obtain low-intensity, countable beams. Typical counting rates were (1–4) $\times10^3$ counts/sec.

2. *Method II: Faraday Cup*

Method II for analyzing the particles (refer to Fig. 2) was used to obtain low-energy ($E \leq 10$ keV/nucleon) total-loss cross sections. Ionization cross sections and excited-state populations cannot be obtained by this method.

This method required a third gas region (the stripper), which contained H_2 gas held at a constant pressure, to ionize the H_2 molecules transmitted through the target. The resulting H_2^+ beam exiting from the stripper was proportional to the H_2 beam transmitted through the target and was deflected to a Faraday cup. The resulting signal was fed to an electrometer whose output was sent to an integrator.

For this method the ion source was operated in the PIG mode to obtain higher beam intensities, measurable by a Faraday cup. Typical H_2^+ currents measured by the final Faraday cup ranged from 10^{-13} to 10^{-10} A.

IV. DATA ANALYSIS

A. Total-Loss Cross Sections and Excited Fractions (Method I)

For this measurement an electric field of about 8 kV/cm was applied transverse to the beam within the target cell in order to deflect the charged collision products from the beam as they formed. We neglect excitation and deexcitation collisions (see Appendix B). The equations that describe the surviving H_2 molecules are

$$F(\pi_t) = [1 - f(\pi_n)]\, e^{-\sigma_t \pi_t} \quad , \tag{1a}$$

$$F^*(\pi_t) = f(\pi_n)\, e^{-\sigma_t^* \pi_t} \quad , \tag{1b}$$

where $F(\pi_t)$ is the number of ground-state $H_2(^1\Sigma_g^+)$ molecules in the beam, after traversing a target thickness π_t, per H_2 molecule incident on the target cell; $F^*(\pi_t)$ is the number of excited $H_2(^3\Pi_u)$ molecules in the beam, after traversing a target thickness π_t, per H_2 molecule incident on the target cell; $f(\pi_n)$ is the fraction of the incident H_2 molecules in the $^3\Pi_u$ state, produced by electron capture by H_2^+ ions in a neutralizer of thickness π_n; and σ_t, σ_t^* are the total-loss cross sections for the $^1\Sigma_g^+$ (ground) and $^3\Pi_u$ states.

The detector system is not capable of distinguishing between the two classes of molecules; therefore we measured the sum $y(\pi_t) = F(\pi_t) + F^*(\pi_t)$ for several target thicknesses π_t. Figure 4 shows the quantity $y(\pi_t)$ versus target thickness for a 50-keV

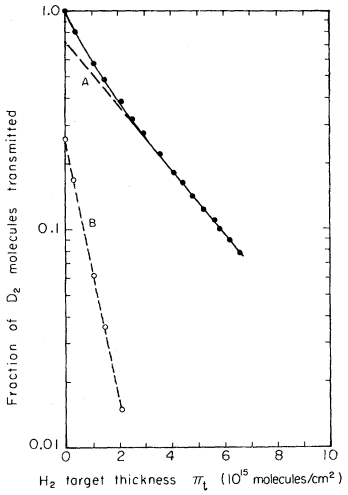

FIG. 4. Observed attenuation of a beam of D_2 molecules in an H_2 target by method I. The molecules were produced in a Mg neutralizer (thin target) by electron capture by 50-keV D_2^+. The solid line is the result of a least-squares fit of the data to the sum of two exponentials. Curve A is an extrapolation of the thick-target asymptote; curve B is the difference between the data and curve A. Solid circles are experimental points; open circles are derived points.

D_2 beam produced in a thin-target Mg neutralizer (i.e., single-collision conditions applied) by electron capture by D_2^+ ions. The solid line is the result of a least-squares fit of the data to $y(\pi_t)$. The nonlinear portion is due to the presence of $H_2(^3\Pi_u)$ molecules which attenuate faster than ground-state molecules ($\sigma_t^* > \sigma_t$). As the target thickness increases the attenuation becomes linear on the semilogarithmic plot, reflecting the loss of essentially all $^3\Pi_u$ molecules in the target cell and the transmission of only $^1\Sigma_g^+$ molecules. By subtracting the extrapolated portion (curve A) of the linear region from the data we obtain the lower straight line (curve B) which is the $H_2(^3\Pi_u)$ attenuation. The straight lines are represented by the equations

$$\ln F(\pi_t) = -\sigma_t \pi_t + \ln[1 - f(\pi_n)] \quad \text{(curve A)}, \tag{2a}$$

$$\ln F^*(\pi_t) = -\sigma_t^* \pi_t + \ln f(\pi_n) \quad \text{(curve B)}. \tag{2b}$$

The cross sections are therefore easily obtained from the slopes as

$$\sigma_t = -\Delta \ln F(\pi_t)/\Delta\pi_t , \tag{3a}$$

$$\sigma_t^* = -\Delta \ln F^*(\pi_t)/\Delta\pi_t . \tag{3b}$$

Also, the intercept of curve B yields the fraction of the beam in the $^3\Pi_u$ state, since from Eq. (1b) we have

$$F^*(0) = f(\pi_n) . \tag{4}$$

When the thickness of the Mg-vapor neutralizer was increased to large values ($\pi_n \gtrsim 1\times10^{16}$ atoms/cm^2) or when H_2 or N_2 gas was used as a neutralizer, only a simple exponential attenuation was observed, i.e., $F^*(0) = 0$. The decrease in the $^3\Pi_u$ component with increasing Mg-vapor-neutralizer thickness reflects its larger total-loss cross section. In the case of the H_2 and N_2 gas neutralizers, the absence of detectable $^3\Pi_u$ molecules is due to the large ground-state electron-capture process.

When the H_2 beam contained no $^3\Pi_u$ component, the resulting simple-attenuation curve had the same slope as curve A of Fig. 4, as expected. This enabled us to get an independent measurement of σ_t.

B. Total-Loss Cross Sections (Method II)

The H_2 beam transmitted through the target cell was passed through the stripper where a fraction of it was ionized ($H_2 \rightarrow H_2^+$). The H_2^+ current was integrated for a preset accumulation of charge at the monitor Faraday cup. The collected charge Q can be expressed as

$$Q(\pi_t) = \alpha_1 [1 - f(\pi_n)] e^{-\sigma_t \pi_t} + \alpha_2 f(\pi_n) e^{-\sigma_t^* \pi_t} , \tag{5}$$

where α_1 and α_2 are constants for a given stripper thickness and reflect the efficiency of producing H_2^+ ions from $H_2(^1\Sigma_g^+)$ and $H_2(^3\Pi_u)$ molecules. The measurement was performed by observing the attenuation of $Q(\pi_t)$ for several target cell thicknesses π_t. Figure 5 shows the quantity $Q(\pi_t)$ (in arbitrary units) vs H_2-target thickness for a D_2^+ beam produced in a thin Mg neutralizer (8.5×10^{13} atoms/cm^2) and transmitted through the H_2 target cell. The nonlinearity of the curve in Fig. 5 is larger than the nonlinearity produced by direct observation of the D_2 molecules (method I) under similar conditions (cf. Fig. 4). This is due to the fact that the cross section for D_2^+ production from $D_2(^3\Pi_u)$ is larger than that from $D_2(^1\Sigma_g^+)$, i.e., $\alpha_2 > \alpha_1$. Without a knowledge of α_1 and α_2, we cannot determine $f(\pi_n)$, but we still are able to determine σ_t and σ_t^*. The analysis of the data to yield values for σ_t and σ_t^* is identical to method I.

C. Ionization Cross Sections

With our experimental arrangement we were able to study one of the processes that contribute to the total loss of H_2 molecules: collisional ionization, $H_2 \rightarrow H_2^+$. For this measurement the transverse electric field in the target cell was turned off so that the H_2^+ component in the beam owing to the ionization of H_2 could be measured. Detection of the emerging H_2^+ ions and H_2 molecules was performed by single-particle counting techniques (method I).

Under thin-target conditions the collision relation governing the H_2^+ component F^+ in the beam, owing to the ionization of H_2 ($^1\Sigma_g^+$) and H_2 ($^3\Pi_u$) in the target cell, may be written as

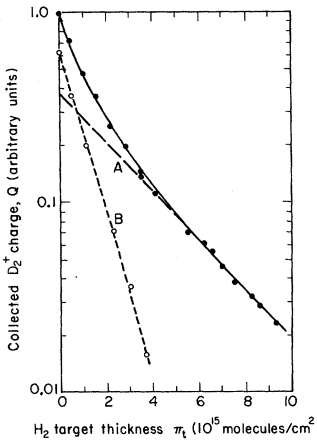

FIG. 5. Observed attenuation of a beam of D_2 molecules in an H_2 target by method II. The figure is a plot of the collected D_2^+ charge Q measured by the Faraday cup after the stripper vs H_2 target gas thickness π_t. The D_2^+ ions were produced by ionization of D_2 in the H_2 target (stripper) $\sim 2\times 10^{14}$ molecules/cm^2 thick. The D_2 molecules were produced by electron capture of 62-keV D_2^+ ions in a Mg-vapor target (neutralizer) of thickness 8.5×10^{13} atoms/cm^2. Curve A is an extrapolation of the thick-target asymptote; curve B is the difference between the data and curve A. Solid circles are experimental points; open circles are derived points.

$$\frac{d}{d\pi_t}F^+(\pi_t) = (\sigma_{H_2^+})F(\pi_t) + (\sigma^*_{H_2^+})F^*(\pi_t)\ , \tag{6}$$

where $\sigma_{H_2^+}$ and $\sigma^*_{H_2^+}$ are the cross sections for ionization ($H_2 \rightarrow H_2^+$ and $H_2^* \rightarrow H_2^+$). In terms of the fraction of excited H_2 molecules, f, this equation yields

$$F^+(\pi_t) = \{(\sigma_{H_2^+})[1 - f(\pi_n)] + (\sigma^*_{H_2^+})f(\pi_n)\}\pi_t\ . \tag{7}$$

Figure 6 is a plot of $F^+(\pi_t)$ vs π_t.

When the incoming H_2 molecules contained no observable fraction of $^3\Pi_u$ states, the slope of the linear relation between $F^+(\pi_t)$ and π_t yielded $\sigma_{H_2^+}$ (curve B). When the H_2 beam did contain an observable fraction of $^3\Pi_u$ molecules (thin Mg neutralizer), the same technique yielded the composite cross section

$$(\sigma_{H_2^+})[1 - f(\pi_n)] + (\sigma^*_{H_2^+})f(\pi_n)$$

[curve A: see Eq. (7)]. Using the value of $f(\pi_n)$ from independent attenuation measurements (see Sec. IV A) for the same neutralizer conditions, the cross section for ionization of the $^3\Pi_u$ state, $\sigma^*_{H_2^+}$, can be determined.

D. Particle Yields

The present section describes the measurement of the particle yields due to energetic H_2^+ ion collisions with Mg vapor. For this measurement the Mg oven was moved to the target cell position. This was done in order to ensure complete collection of the breakup products. (No attempt was made to distinguish between ground-state and excited H_2.) The exit aperture of the oven was enlarged until there was no observable change in the measured beam components for our thickest target. The final oven collimation was 0.33-mm entrance diam and 2.8-mm exit diam. The diameter of the particle detectors (25.4 mm) was larger than the maximum possible beam spreading which is defined by the oven collimation. For this measurement the Mg-vapor thickness was varied from 2×10^{14} to 1×10^{16} atoms/cm^2.

The measurements were performed by passing H_2^+ ions through the oven for several Mg-vapor thicknesses and counting the exiting H_2^+, H^+, H, and H_2 components of the beam. This enabled us to obtain the yields of the reactions

$$H_2^+ + Mg \rightarrow H_2 - e + \cdots, \tag{8}$$

$$H_2^+ + Mg \rightarrow H + H - e + \cdots\ , \tag{9}$$

$$H_2^+ + Mg \rightarrow H + H^+ + \cdots\ , \tag{10}$$

$$H_2^+ + Mg \rightarrow H^+ + H^+ + e + \cdots\ . \tag{11}$$

(The H^- yield was measured at 20 keV/nucleon and was found to be negligible. We expect the H^- yield to peak at energies less than those used in the present work.)

In order to separate the H_2 and H + H contributions, the neutral particles had to be detected once with the mesh in and once with it out. From these measurements we were able to account for the total

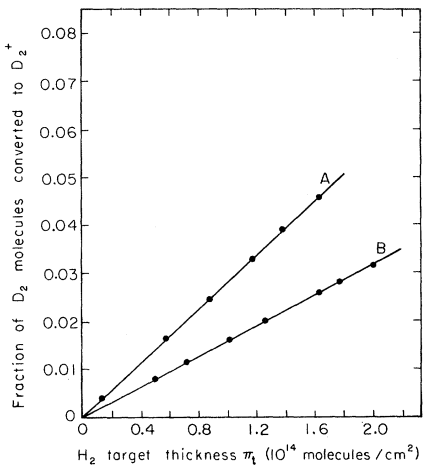

FIG. 6. Production of D_2^+ ions from the ionization of 60-keV D_2 molecules in collision with a H_2 gas target. The D_2 molecules were produced by electron capture by D_2^+ ions in a Mg-vapor neutralizer. Line A connects the experimental data using a thin Mg-vapor neutralizer ($\pi_n \lesssim 1\times 10^{14}$ atoms/cm^2); line B connects the experimental data using a thick Mg-vapor neutralizer ($\pi_n \gtrsim 1\times 10^{16}$ atoms/cm^2).

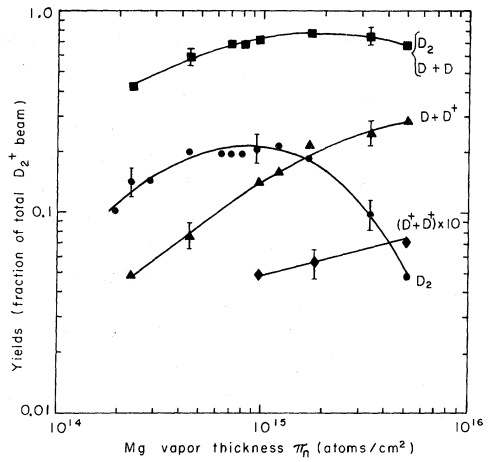

FIG. 7. The observed dependence on the Mg-vapor-target thickness π_n of the particle yields from the collisional breakup of D_2^+. The beam energy was 10 keV/nucleon. ■, $D_2^+ + Mg \rightarrow D_2 - e + \cdots$, $D + D - e + \cdots$; ●, $D_2^+ + Mg \rightarrow D_2 - e + \cdots$; ▲, $D_2^+ + Mg \rightarrow D + D^+ + \cdots$; ◆, $D_2^+ + Mg \rightarrow D^+ + D + e + \cdots$. The lines drawn through our points are to guide the eye and have no other significance.

beam and calculate the individual beam-component fractions.

E. Error Analysis

For all experimental results of this work, the assignment of uncertainty is based on the reproducibility of the data occurring in a number of runs taken months apart, on the standard deviation of the least-squares fit of the data, and on systematic experimental errors. The long-term reproducibility of the ground-state measurements was ±5% with a standard deviation of the least-squares fit of the data of ±3%. This was true in both methods I and II, although for $E \geq 20$ keV/nucleon the results using the stripper–Faraday-cup combination for detection (method II) were consistently 9% lower than the results using single-particle counting techniques (method I). A possible explanation for the difference in the results is that the vibrational population distribution of the ions was not the same in the two cases because of the different modes of ion-source operation.

For the excited-state measurements, the long-term reproducibility was ±17%, and the standard deviation of the least-squares fit of the data varied from ±5 to ±20%. Statistical errors in counting were always less than 4% and in all but a few cases less than 1%. Possible systematic experimental uncertainties resulting from pressure and target-length measurements are estimated to total about ±7%.

The effect of collimator interceptions and gas background were determined to be negligible since the fraction of the H_2 beam surviving with no target gas was always >0.998. Other possible sources of error which are determined to be inconsequential in this work are target and source gas contamination and detector signals of unknown origin that were modulated with the beam.[16]

To experimentally investigate the possibility of the presence of unknown systematic errors, we measured the well-known single-electron-capture cross section for energetic protons in collision with H_2 gas in the (10–30)-keV energy range. Our measurements agree to within ±5% with those of Stier and Barnett.[19] We also measured the total-loss cross section for energetic hydrogen atoms passing through H_2 gas. These results also agreed to within ±5% with those of Ref. 19.

The estimated absolute uncertainty in the present results ranges from ±18 to ±25% for the excited-state cross sections and populations (those that survive for $t \gtrsim 0.5$ μsec), is ±10% for the ground-state cross sections, and ranges from ±10 to ±15% for the particle-yield measurements. The confidence level associated with these uncertainties is estimated to be 60%. The assigned absolute uncertainty for each data point may be found with the tabulated data in Sec. V.

V. RESULTS AND DISCUSSION

A. Beam Populations

1. *Yields of Atoms and Molecules from Collisions of H_2^+ Ions in* Mg *Vapor*

The data plotted in Fig. 7 show the variation with Mg-vapor thickness of the experimental yields of reaction products due to 10-keV/nucleon D_2^+ ion collisions with Mg vapor. We see that at 10 keV/nucleon, with $\pi_n \sim 2\times10^{15}$ atoms/cm^2, approximately 90% of the incident H_2^+ ions have been converted to neutrals, and the reaction $H_2^+ + Mg \rightarrow H + H - e + \cdots$ is the dominant inelastic process.

In Fig. 8 we illustrate the variation, with Mg-vapor thickness and with H_2^+ particle energy, of the experimental H_2 yields $\mathfrak{F}$ from H_2^+ ion collisions with Mg vapor. The maximum H_2 yields occur around 10^{15} atoms/cm^2 for all energies measured and increase with decreasing energy. Also shown in the figure are the results of Kingdon *et al.* at 20 keV/nucleon.[20]

No H_2^- or D_2^- ions were observed. Analysis of the yields allows us to assign an upper bound of 10^{-21} cm^2/atom to the cross section for double electron capture into H_2^- states with lifetimes longer than $\sim 10^{-7}$ sec. The H^- yield at 20 keV/nucleon was observed to be less than 1% for $\pi_n \lesssim 10^{15}$ atoms/cm^2.

2. *Yields of $^3\Pi_u$ Molecules from Collisions of H_2^+ Ions in* Mg *Vapor*

The results shown in Fig. 9 illustrate the variation with Mg-vapor thickness and with H_2^+ particle

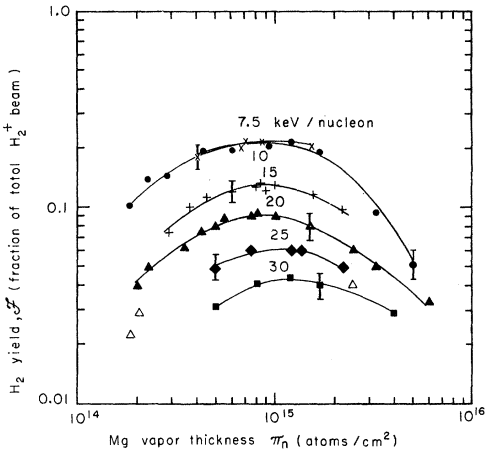

FIG. 8. Fraction of incident H_2^+ ions converted to H_2 molecules vs Mg-vapor thickness π_n. Solid symbols, present work; open symbols, Ref. 20; ×, 7.5 keV/nucleon; ●, 10 keV/nucleon; +, 15 keV/nucleon; △, ▲, 20 keV/nucleon; ◆, 25 keV/nucleon; ■, 30 keV/nucleon. (For $E < 20$ keV/nucleon the incident projectile was D_2^+.) The lines through the points are drawn in to guide the eye and have no other significance.

energy of the measured fraction f of the H_2 molecules formed in the $^3\Pi_u$ state by electron capture by H_2^+ ions in Mg vapor. We see from Fig. 9 that, for $\pi_n \lesssim 2\times10^{14}$ atoms/cm^2, f is independent of target thickness, i.e., single-collision conditions exist, and it is a slowly decreasing function of energy.

From calculations for electron capture into the $n = 2$ level by protons from Mg,[7] we expect up to 50% of the electron capture by H_2^+ from Mg to be into the $n = 2$ H_2 ($^3\Pi_u$) state at the lower end of our energy range. For the broad rotational population distribution anticipated for our ion source, we also estimate that approximately one-half of the $^3\Pi_u$ molecules formed are susceptible to predissociation (Sec. II). Our thin-target results for f (which vary from 0.36 at 11.2 keV/nucleon to 0.23 at 35 keV/nucleon) are consistent with these estimates.

When the results for f were compared at equal H_2^+, D_2^+, and HD^+ velocities (at 15 and 20 keV/nucleon), no differences were observed, within experimental uncertainties. Since the nuclear symmetry associated with H_2 and D_2 breaks down for the heteronuclear isotopic molecule HD, the equivalence of the results at equal velocities seems to indicate that the interaction between the electronic and rotational motion is small. In this case the electronic dipole selection rules for homonuclear molecules are very good approximations for heteronuclear molecules.[11,12]

We also looked for a $^3\Pi_u$ component in an H_2 beam prepared by H_3^+ dissociation in thin-target Mg vapor. The H_2 molecules were formed via the reactions

$$H_3^+ + Mg \rightarrow \begin{cases} H_2 + H - e + \cdots \\ H_2 + H^+ + \cdots . \end{cases}$$

This measurement was performed at 7.5 keV/nucleon for two different Mg-vapor thicknesses, 0.9×10^{14} and 2×10^{14} atoms/cm^2. No $H_2(^3\Pi_u)$ molecules were observed.

B. Cross Sections

1. *Total-Loss Cross Sections of* $^1\Sigma_g^+$ and $^3\Pi_u$ H_2 *Molecules in Collisions with* H_2 *Gas*

The total-loss cross sections for the excited state σ_t^* and for the ground state[21] σ_t are given in Table I and in Fig. 10. McClure[22] has obtained the ground-state total-loss cross section at 5 keV/nucleon by a very different technique. His result is in excellent agreement with the present results (see Fig. 10).

We are not aware of any theoretical calculations

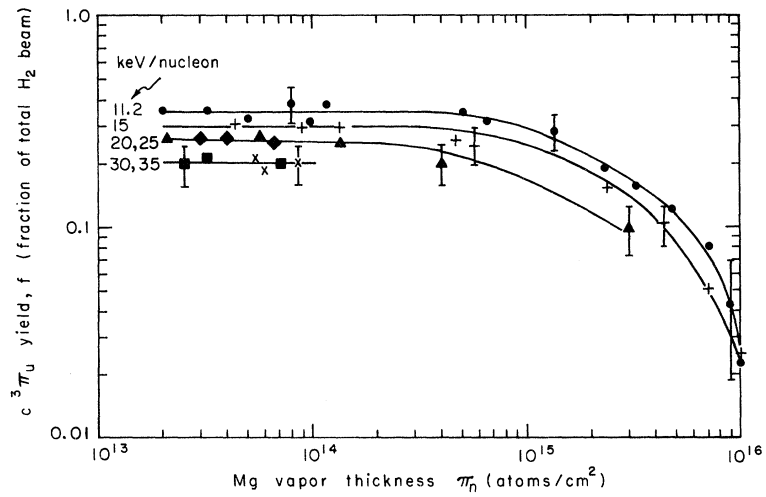

FIG. 9. Fraction of H_2 molecules that are in the $c\,^3\Pi_u$ state vs Mg-vapor thickness π_n. ●, 11.2 keV/nucleon; +, 15 keV/nucleon; ▲, 20 keV/nucleon; ◆, 25 keV/nucleon; ■, 30 keV/nucleon; ×, 35 keV/nucleon. (For $E < 20$ keV/nucleon the incident projectile was D_2^+.) The lines through the points are drawn in to guide the eye and have no other significance.

TABLE I. Total collisional-loss cross sections (in units of 10^{-16} cm^2/molecule) for $H_2(^1\Sigma_g^+)$, σ_t, and $H_2(^3\Pi_u)$, σ_t^*, in H_2 gas. The assigned absolute uncertainties indicated are based on an estimated 60% confidence level. (For $E<20$ keV/nucleon the incident projectile was D_2^+.)

	$\sigma_t(\pm 10\%)$		σ_t^*	
Energy (keV/nucleon)	Particle counting (method I)	Faraday cup (method II)	Particle counting (method I)	Faraday cup (method II)
1.0		1.70		
1.7		1.85		
3.0		2.10		
5.0		2.50		$13.3\ ^{+2.6}_{-2.3}$
7.5		2.70		
8.7		2.80		$13.4\ ^{+2.3}_{-2.4}$
11.2		3.10		14.0 ± 2.5
12.2	3.25		$13.0\ ^{+2.5}_{-2.3}$	
15.0	3.35	3.20	$12.3\ ^{+2.5}_{-2.1}$	$11.7\ ^{+2.4}_{-2.3}$
20.0	3.52		$13.5\ ^{+2.2}_{-2.6}$	
22.5		3.10		$9.3\ ^{+1.6}_{-1.5}$
25.0	3.50	3.18	$10.4\ ^{+1.9}_{-1.8}$	
30.0	3.55	3.15	9.0 ± 2.2	$8.2\ ^{+1.8}_{-1.4}$
35.0	3.50		$8.1\ ^{+1.8}_{-1.4}$	
42.0	3.50	3.15		$7.6\ ^{+1.8}_{-1.6}$

to compare with the present results.

2. *Ionization Cross Sections of* $^1\Sigma_g^+$ and $^3\Pi_u$ H_2 *Molecules in Collisions with* H_2 *Gas*

One of the cross sections contributing to the total-loss cross section, that for ionization ($H_2 \rightarrow H_2^+$), has also been determined for both the $^1\Sigma_g^+$ state $\sigma_{H_2^+}$ and the $^3\Pi_u$ state $\sigma^*_{H_2^+}$ in H_2 gas. The results are presented in Table II and in Fig. 11. For the ground-state ionization cross section we see from Fig. 11 that the experimental results of McClure[22] are in excellent agreement with the present results over the entire energy range investigated. Again, we know of no theoretical calculations to compare with these results.

VI. SUMMARY AND CONCLUSIONS

The cross sections for the total loss and ionization of $H_2(^1\Sigma_g^+)$ [$1 \leq E$ (keV/nucleon) ≤ 42] and $H_2(^3\Pi_u)$ molecules [$5 \leq E$ (keV/nucleon) ≤ 42] in collisions with H_2 gas have been measured. The result of McClure[22] at 5 keV/nucleon for the total-loss cross section of the $^1\Sigma_g^+$ state is in excellent agreement with the present measurements. The data of McClure for the ionization cross section of the $^1\Sigma_g^+$ state are also in excellent agreement. We have not found any data on collisional cross sections for the $^3\Pi_u$ state to compare with present results.

The four cross sections measured in the pres-

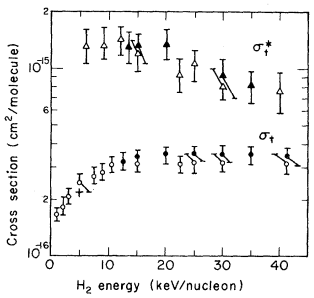

FIG. 10. Total-loss cross sections for collisions of energetic $H_2(\Sigma_g^+)$, σ_t, and $H_2(^3\Pi_u)$, σ_t^* with H_2 gas. Present results: triangles, σ_t^*; circles, σ_t. Solid symbols, particle counting technique (method I); open symbols, Faraday cup technique (method II). (For $E<20$ keV/nucleon the incident projectile was D_2^+.) The result of McClure (Ref. 22) at 5 keV/nucleon for σ_t is indicated by +.

ent work ($\sigma_{H_2^+}$, $\sigma^*_{H_2^+}$, σ_t, σ^*_t) vary gradually over the energy range of the measurements. The excited-state cross sections range from two to five times larger than the ground-state cross sections. The contribution of the ionization cross section to the total-loss cross section, both for the ground and excited states, increases from ~30 to ~60% as the energy increases over the present range.

The data agreed, within experimental uncertainties, using H_2^+, D_2^+, and HD^+ ions of equal velocity. This suggests that for the $^3\Pi_u$ molecular state strong coupling between the nuclear rotation and the electronic motion does not exist.

We have measured the $H_2(^3\Pi_u)$ yields due to collisions of H_2^+ ions in Mg vapor. From the results it can be shown that 6.5% of the incident H_2^+ beam can be converted to $H_2(^3\Pi_u)$ molecules at 11.2 keV/nucleon using an optimized Mg-vapor-target thickness $\sim 7\times10^{14}$ atoms/cm^2. This yield is a steeply decreasing function of energy (decreasing to 1.8% at 20 keV/nucleon) owing to the rapid decrease in the total production of H_2 molecules rather than to a significant change in the fraction of the H_2 molecules in the $^3\Pi_u$ state. The fraction of the H_2 molecules in the $^3\Pi_u$ state varies slowly over the present energy range from 36% at 11.2 keV/nucleon to 23% at 35.0 keV/nucleon for Mg-vapor thicknesses less than $\sim 1\times10^{14}$ atoms/cm^2. We have found no significant $^3\Pi_u$ yields for Mg-vapor-neutralizer thicknesses greater than $\sim 1\times10^{16}$ atoms/cm^2, nor for H_2 or N_2 neutralizers. These results are consistent with estimates by Hiskes.[7]

The presence of $H_2(^3\Pi_u)$ molecules from the dissociation of H_3^+ ions in Mg vapor has not been observed. Also, no H_2^- ions were observed from the passage of H_2^+ ions through Mg vapor. This observation has allowed us to place an upper bound of 10^{-21} cm^2/atom on the cross section for double electron capture into H_2^- states with lifetimes longer than $\sim 10^{-7}$ sec by 7- to 20-keV/nucleon H_2^+ ions in collision with Mg vapor.

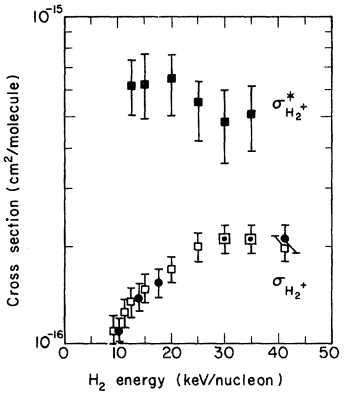

FIG. 11. Cross sections for the ionization of energetic $H_2(^1\Sigma_g^+)$, $\sigma_{H_2^+}$, and $H_2(^3\Pi_u)$, $\sigma_{H_2^+}$, in collision with H_2 gas. Present results: solid squares, $\sigma^*_{H_2^+}$; open squares, $\sigma_{H_2^+}$. (For $E<20$ keV/nucleon the incident projectile was D_2^+.) The results of McClure (Ref. 22) for $\sigma_{H_2^+}$ are indicated by solid circles.

TABLE II. Collision cross sections for the ionization of $H_2(^1\Sigma_g^+)$, $\sigma_{H_2^+}$, and $H_2(^3\Pi_u)$, $\sigma^*_{H_2^+}$, in H_2 gas. The assigned absolute uncertainties are based on an estimated 60% confidence level. (For $E<20$ keV/nucleon the incident projectile was D_2^+.) The cross sections, in units of 10^{-16} cm^2/molecule, were obtained by method I.

H_2 energy (keV/nucleon)	$\sigma_{H_2^+}$ (±10%)	$\sigma^*_{H_2^+}$
8.7	1.12	
11.2	1.26	
12.2	1.37	$6.2\,^{+1.2}_{-1.1}$
15.0	1.48	$6.2\,^{+1.5}_{-1.3}$
20.0	1.70	$6.5\,^{+1.2}_{-1.5}$
25.0	2.0	$5.5\,^{+0.9}_{-1.3}$
30.0	2.1	4.8 ± 1.2
35.0	2.1	$5.1\,^{+1.1}_{-1.2}$
42.0	2.0	

As shown in the present work, measurements using H_2 beams that have been prepared from H_2^+ collisions in Mg vapor are sensitive to the vapor pressure, because this determines the $^3\Pi_u$ fraction in the beam. Such beams must be treated in terms of two states, each of which has a different attenuation cross section. For example, Solov'ev *et al.*[14] obtained H_2^+ electron-capture cross sections in Mg vapor by a process that involved the conversion of H_2 molecules to H_2^+ ions in a He stripper cell. Without any information about the existence of $^3\Pi_u$ molecules in the beam, they analyzed their data by using only ground-state-ionization cross sections. Estimates based on the results of the present experiment show that the H_2^+ electron-capture cross sections obtained in Ref. 14 could be too large by as much as a factor of 2.

We expect that H_2 beams, prepared by passage of H_2^+ ions through other low-ionization-potential vapors such as Li, Cs, Na, and K, would contain large fractions of $H_2(^3\Pi_u)$ molecules.

More detailed results for the yields of H_2, H, and H^+ from collisions of H_2^+ ions in Mg vapor and the use of $^3\Pi_u$ beams in neutral-injection controlled-fusion experiments will be reported elsewhere.

ACKNOWLEDGMENTS

We are grateful to Dr. John R. Hiskes for sug-

gesting this work and for many useful and stimulating theoretical discussions. The skillful experimental assistance of J. W. Stearns is greatly appreciated. V. J. Honey provided invaluable assistance in the construction and maintenance of the electronic equipment. One of us (T. J. M.) held a U. S. AEC Nuclear Science and Engineering Fellowship during part of this work.

APPENDIX A: EXCITED STATES OF H_2 MOLECULE

In this appendix we survey the pertinent electronic excited states of H_2 to determine which excited states have lifetimes greater than $\sim 10^{-6}$ sec. For the present discussion we can divide the excited states into three groups: (i) highly excited states ($n \gtrsim 8$), (ii) intermediate-excited states ($n \lesssim 8$), and (iii) low-lying states having excitation energies less than ~ 12.5 eV.

First, we address ourselves to groups (i) and (ii). Since the excited electrons in H and H_2 move in approximately the same potential, they will have approximately the same radiative lifetimes. From the theoretical work of Hiskes, Tarter, and Moody,[23] we find that the atomic hydrogen states with $n \gtrsim 8$, group (i), have lifetimes which are greater than $\sim 10^{-6}$ sec. For group (ii) it can be shown that these intermediate states decay in times shorter than $\sim 10^{-6}$ sec to lower states,[23] and further, that no anomalies resulting in longer than normal lifetimes are expected.[11]

We now turn our attention to group (iii) (the H_2 excited states shown in Fig. 1 comprise this group). Lichten[24] first verified the existence of metastable molecular hydrogen by use of the atomic-beam magnetic-resonance technique. Specifically, he found that the lowest vibrational level ($v = 0$) of the $c\,^3\Pi_u$ state of H_2 is metastable, i.e., does not radiatively decay by electric dipole transitions. Recently, Brooks *et al.*[25] have found experimental evidence which leads them to conclude that there is at least one additional long-lived level of the $c\,^3\Pi_u$ state other than the $v = 0$ level. They conclude that the level is most likely, but not conclusively, the $v = 1$ level. The Kronig selection rules for an allowed radiative transition in a diatomic system[26] show that the $c\,^3\Pi_u$ ($v = 0$ level), although not able to decay via electric dipole transitions, can decay radiatively by magnetic dipole, electric quadrupole, or higher moment emissions to the $b\,^3\Sigma_u^+$ state [the $b\,^3\Sigma_u^+$ state is repulsive and dissociates into two ground-state H atoms in $\sim 10^{-14}$ sec (Ref. 24)]. The radiative lifetime for these transitions has been estimated by Freis and Hiskes[27] to be 10^{-3} sec for H_2, and recently Johnson[28] has obtained experimental values of $\sim 10^{-3}$ sec for H_2, D_2, and HD. Freis and Hiskes[27] have also calculated the electric-dipole radiative lifetimes for the $c\,^3\Pi_u$, $v > 0$, levels decaying to the only allowable final state, $a\,^3\Sigma_g^+$ [this state has been calculated to decay to the $b\,^3\Sigma_u^+$ state in $\sim 10^{-8}$ sec (Ref. 29)]. Their calculated times are about 10^{-4} sec or longer for all vibrational levels. Thus we conclude that all vibrational states of $c\,^3\Pi_u$ have radiative lifetimes greater than 10^{-4} sec.

We now turn our attention to predissociation, the nonradiative transition process in diatomic molecules.[30] The $c\,^3\Pi_u$ state is susceptible to perturbations from the repulsive $b\,^3\Sigma_u^+$ state when the potential energy functions of these states come close enough together so that an overlapping of wave functions exists and causes a nonzero matrix element for predissociation. There are two types of predissociation of the $c\,^3\Pi_u$ state: allowed, induced by rotational-electronic perturbations; and forbidden, induced by spin-orbit and spin-spin couplings. The selection rules governing predissociation[11] indicate that, although there are many states close to the $c\,^3\Pi_u$ state, predissociation can take place only via the $b\,^3\Sigma_u^+$ state.

As has been pointed out by Kronig,[31] under very strong coupling conditions allowed predissociation lifetimes could be as short as 10^{-11} sec. Lichten,[32] in order to explain his experimental observations, has concluded that for the $c\,^3\Pi_u$ state allowed predissociation lifetimes are $\sim 10^{-9}$ sec. Herzberg,[33] based on experiments dealing with the absorption spectrum in the visible region of H_2 excited by a flash discharge, has estimated an upper bound of $\tau = 0.3$ μsec on the lifetime for allowed predissociation of the $v = 2$ level of $c\,^3\Pi_u$. Also, owing to the change in proximity of the $b\,^3\Sigma_u^+$ and $c\,^3\Pi_u$ potential-energy states with changes in internuclear separation, we expect the predissociation lifetime to decrease with increasing vibrational excitation of the $c\,^3\Pi_u$ state (see Fig. 1). Herzberg[33] has experimentally verified this behavior. Therefore, based on this available information, we bound the allowed predissociation lifetime as follows: nanoseconds $\lesssim \tau \lesssim$ tenths of microseconds.

A survey of the selection rules for allowed predissociation shows that half of the rotational states of the $c\,^3\Pi_u$ molecule are susceptible to this loss mechanism.[11]

Finally, Bottcher[34] and Chiu[35] have performed theoretical calculations on the forbidden predissociation lifetimes and concluded that they are of the order of 10^{-3} sec, while Lichten has experimentally measured lifetimes ranging from 0.1×10^{-3} to 0.5×10^{-3} sec.[32]

Hence, we conclude that all the levels of the $c\,^3\Pi_u$ state have radiative lifetimes longer than $\sim 10^{-6}$ sec, but half of their rotational states are likely to undergo allowed predissociation within this time.

We now consider the remaining low-lying excited states of H_2 (see Fig. 1). The $a\,^3\Sigma_g^+$ state has been

shown to decay to the $b\,^3\Sigma_u^+$ state in $\sim 10^{-8}$ sec.[29] Also, the $B\,^1\Sigma_u^+$ and the $C\,^1\Pi_u$ states have both been shown to decay by allowed transitions in $(8\pm2)\times10^{-10}$ sec and $(6\pm2)\times10^{-10}$ sec, respectively.[36] This is not the case, however, for the $n=2\,^1\Sigma_g^+$ state. Davidson[37] has studied this state and computed the potential curve. He finds the potential function to contain two minima: the $E\,^1\Sigma_g^+$ state at $R=1.0$ Å, and the $F\,^1\Sigma_g^+$ state at $R=2.27$ Å. Wolniewicz[38] has calculated the transition probabilities for the $F\,^1\Sigma_g^+$-$B\,^1\Sigma_u^+$ transition and finds approximately half the transitions of the F-B band to have lifetimes greater than 10^{-5} sec. For comparable transitions of the E-B band we conclude, based on Wolniewicz's calculation of the band strengths, that the lifetimes are $<10^{-8}$ sec.

In summary, we conclude that the $c\,^3\Pi_u$ and $F\,^1\Sigma_g^+$ states and the $n\gtrsim8$ states have lifetimes long enough to allow them to traverse typical apparatus lengths and must be considered in the interpretation of our experimental results.

APPENDIX B: EFFECTS OF COLLISIONAL EXCITATION AND DEEXCITATION OF THE PRESENT MEASUREMENTS

The analysis of the H_2 attenuation curves in Sec. IV A is based on the assumption that the loss processes remove H_2 molecules from the beam. This, of course, is not true for collisions which shuffle the populations of the ground and $^3\Pi_u$ state, i.e., excitation from $^1\Sigma_g^+$ to $^3\Pi_u$ or deexcitation from $^3\Pi_u$ to $^1\Sigma_g^+$. Both of these processes require a change in spin, which can be achieved only in an exchange collision in which one electron is ejected and another captured. This is an unlikely process in our energy range.

The fact that excitation and deexcitation collisions do not affect the attenuation analysis in the case of triplet excited states has been demonstrated by Gilbody *et al.*[39] for He ($2\,^3S$). Since the effect of the above processes should be a function of the ionization potential of the target gas used, the measured value of the excited-state population should also depend on the target. Gilbody *et al.*[39] used a wide variety of gases with no observable change in the metastable excited-state populations. They concluded that over their energy range (7.5–87.5 keV/nucleon) collisional deexcitation of He ($2\,^3S$) was not important.

Although we did not carry out a systematic study of the $c\,^3\Pi_u$ fraction in the H_2 beam as a function of target gas, one other target was used so as to experimentally convince ourselves of the above arguments. The vapor of C_6H_6 was chosen as the target, because its ionization potential is less than the excitation energy of the $H_2(^3\Pi_u)$ state (9.6 and 11.9 eV, respectively), thus permitting Penning ionization to occur. That is, the reaction $H_2(^3\Pi_u)+C_6H_6 \rightarrow H_2(^1\Sigma_g^+)+(C_6H_6)^+ + e$ is energetically possible; this greatly increases the available final-state phase space and so enhances the deexcitation probability.

If we are unable to observe a change in the measured value of the $^3\Pi_u$ fraction by using C_6H_6, we may assume that within the accuracy of the measurements there are no effects occurring which our detectors are not capable of "seeing." No change in the $^3\Pi_u$ fraction was observed at 22.5 keV/nucleon.

As part of this investigation we have also measured the total-loss cross sections in C_6H_6. We obtained $\sigma_t^* = (3.50\pm0.90)\times10^{-14}$ and $\sigma_t = (1.55\pm0.25)\times10^{-15}$ cm^2/molecule.

We note two other possibilities for collisional deexcitation: collisional mixing of the $c\,^3\Pi_u$ state and its neighboring $a\,^3\Sigma_g^+$ state, with subsequent decay in $\sim 10^{-8}$ sec to the $b\,^3\Sigma_u^+$ state,[29] or collisional mixing causing the transition of $c\,^3\Pi_u$-$b\,^3\Sigma_u^+$ directly. But the $b\,^3\Sigma_u^+$ state is repulsive and dissociates to two ground state atoms in $\sim 10^{-14}$ sec,[24] thereby causing the loss of the H_2 molecule from the beam. This loss process is included in the total-loss cross section that is measured from the attenuation data and, therefore, does not affect the analysis in Sec. IV.

---

*Work performed under the auspices of the U. S. Atomic Energy Commission.

†Present address: Department of Pure and Applied Physics, The Queen's University, Belfast, Northern Ireland.

[1]H. S. W. Massey and E. H. S. Burhop, *Electronic and Ionic Impact Phenomena* (Oxford U. P., London, 1956), Chap. VII, p. 441.

[2]A. H. Futch and C. C. Damm, Nucl. Fusion 3, 124 (1963).

[3]W. Haeberli, Ann. Rev. Nucl. Sci. 17, 373 (1965).

[4]R. N. Il'in, V. A. Oparin, E. S. Solov'ev, and N. V. Fedorenko, *Fourth International Conference on the Physics of Electronic and Atomic Collisions, Quebec*, 1965 (Science Bookcrafters, Hastings-on-Hudson, N. Y., 1965), p. 315.

[5]K. H. Berkner, W. S. Cooper III, S. N. Kaplan, and R. V. Pyle, Phys. Rev. 182, 103 (1969).

[6]V. A. Oparin, R. N. Il'in, and E. S. Solov'ev, Zh. Eksperim. i Teor. Fiz. 52, 369 (1967)[Sov. Phys. JETP 25, 240 (1967)].

[7]J. R. Hiskes, Phys. Rev. 180, 146 (1969).

[8]J. R. Hiskes, Bull. Am. Phys. Soc. 13, 308 (1968).

[9]H. B. Gilbody, R. Browning, and G. Levy, J. Phys. B 1, 230 (1968).

[10]T. J. Morgan, K. H. Berkner, and R. V. Pyle, Phys. Rev. Letters 26, 602 (1971).

[11]G. Herzberg, *Spectra of Diatomic Molecules* (Van Nostrand, New York, 1950).

[12]R. H. Garstang, in *Atomic and Molecular Processes*, edited by D. R. Bates (Academic, New York, 1962), p. 19.

[13]J. Kingdon, M. Payne, and A. C. Riviere, UKAEA

Culham Laboratory Report No. CLM-PR11, 1968, p. B.23 (unpublished).

[14]E. S. Solov'ev, R. N. Il'in, V. A. Oparin, and N. V. Fedorenko, Zh. Eksperim. i Teor. Fiz. 53, 1933 (1967) [Sov. Phys. JETP 26, 1097 (1968)].

[15]J. R. Hiskes, Nucl. Fusion 2, 38 (1962).

[16]A more detailed description of the apparatus can be found in Thomas J. Morgan, Lawrence Berkeley Laboratory Report No. LBL-394, 1971 (unpublished).

[17]Klaus H. Berkner, Robert V. Pyle, and J. Warren Stearns, Phys. Rev. 178, 248 (1969).

[18]Ralph R. Hultgren, Raymond L. Orr, and Kenneth K. Kelly, supplement to Ralph R. Hultgren, Raymond L. Orr, Philip D. Anderson, and Kenneth K. Kelly, *Selected Values of Thermodynamic Properties of Metals and Alloys* (Wiley, New York, 1963); and R. R. Hultgren (private communication).

[19]P. M. Stier and C. F. Barnett, Phys. Rev. 103, 896 (1956).

[20]J. Kingdon, M. Payne, and A. C. Riviere, UKAEA Culham Laboratory Report No. CLM-PR10, 1967, p. 56 (unpublished).

[21]The term "ground state" as used here refers to the electronic ground state. It is quite likely that these molecules are in various vibrationally excited states (see discussion in Sec. II).

[22]G. W. McClure, Phys. Rev. 134, A1226 (1964).

[23]J. R. Hiskes, C. B. Tarter, and D. A. Moody, Phys. Rev. 133, A424 (1964); numerical values for both field-free and Stark lifetimes are given in J. R. Hiskes and C. B. Tarter, Lawrence Radiation Laboratory Report No. UCRL-7088 Rev. I, 1964 (unpublished).

[24]W. Lichten, Phys. Rev. 120, 848 (1960).

[25]P. R. Brooks, W. Lichten, and R. Reno, Phys. Rev. A 4, 2217 (1971).

[26]Reference 11, p. 221.

[27]R. P. Freis and J. R. Hiskes, Phys. Rev. A 2, 573 (1970).

[28]C. E. Johnson, Lawrence Berkeley Laboratory Report No. LBL-328, 1971 (unpublished); Phys. Rev. A 5, 1026 (1972).

[29]H. M. James and A. S. Coolidge, Phys. Rev. 55, 184 (1939).

[30]Reference 11, pp. 405–434.

[31]Reference 11, p. 410.

[32]W. Lichten, Bull. Am. Phys. Soc. 7, 43 (1963).

[33]G. Herzberg, Sci. Light 16, 14 (1967).

[34]C. Bottcher, Ph. D. thesis (The Queen's University of Belfast, 1968) (unpublished).

[35]Lue-Yung Chow Chiu, J. Chem. Phys. 40, 2276 (1964).

[36]James E. Hesser, J. Chem. Phys. 48, 2518 (1969).

[37]Ernest R. Davidson, J. Chem. Phys. 35, 1189 (1961).

[38]L. Wolniewicz, J. Chem. Phys. 51, 5002 (1969).

[39]H. B. Gilbody, K. F. Dunn, R. Browning, and C. J. Latimer, J. Phys. B 3, 1105 (1970).

PHYSICAL REVIEW A VOLUME 5, NUMBER 4 APRIL 1972

Onsager Symmetry Relations and the Spectral Distribution of Scattered Light

H. N. W. Lekkerkerker and W. G. Laidlaw

Department of Chemistry, University of Calgary, Calgary 44, Alberta, Canada

(Received 4 November 1971)

The Onsager symmetry relations, used in conjunction with appropriate linear transformations of the hydrodynamic variables, allow one to analyze the distribution of the eigenvalues of the hydrodynamic matrix and to establish symmetry characteristics of its diagonalizing matrices. The implications of these results for the analysis of the spectral distribution of the polarized component of scattered light are pointed out.

I. INTRODUCTION

In recent years there has been considerable activity, both experimentally as well as theoretically, in the study of the spectral distribution of scattered light.[1] The most commonly used approach to calculate the spectrum is based on Onsager's assumption concerning the regression of fluctuations.[2,3] The number of peaks in the spectrum can be established by determining the number of complex eigenvalues of the hydrodynamic matrix. For a more detailed analysis one may undertake a normal-mode decomposition of the spectral distribution. It is the purpose of this paper to show that the Onsager symmetry relations used in conjunction with appropriate linear transformations of hydrodynamic variables allow one to determine the maximum number of complex roots of the hydrodynamic matrix and to establish symmetry characteristics of the diagonalizing matrices. The distribution of eigenvalues establishes that the spectrum of light scattered from an ordinary fluid can have at most three peaks. The symmetry of the diagonalizing matrices of the hydrodynamic matrix results in a simplification in the normal-mode decomposition.

II. SPECTRUM OF SCATTERED LIGHT

As is well known,[4] the spectral-intensity distribution of the polarized component of scattered light $I(\vec{k}, \Omega+\omega)$ is proportional to the scattering function $S_\epsilon(\vec{k}, \omega)$, where $S_\epsilon(\vec{k}, \omega)$ is the spectral density of $\Delta\epsilon(\vec{k}, t)$ the $\vec{k}$th spatial Fourier component of the fluctuation in the local dielectric constant. Here $\vec{k}$ is the change in wave vector, ω the change in fre-